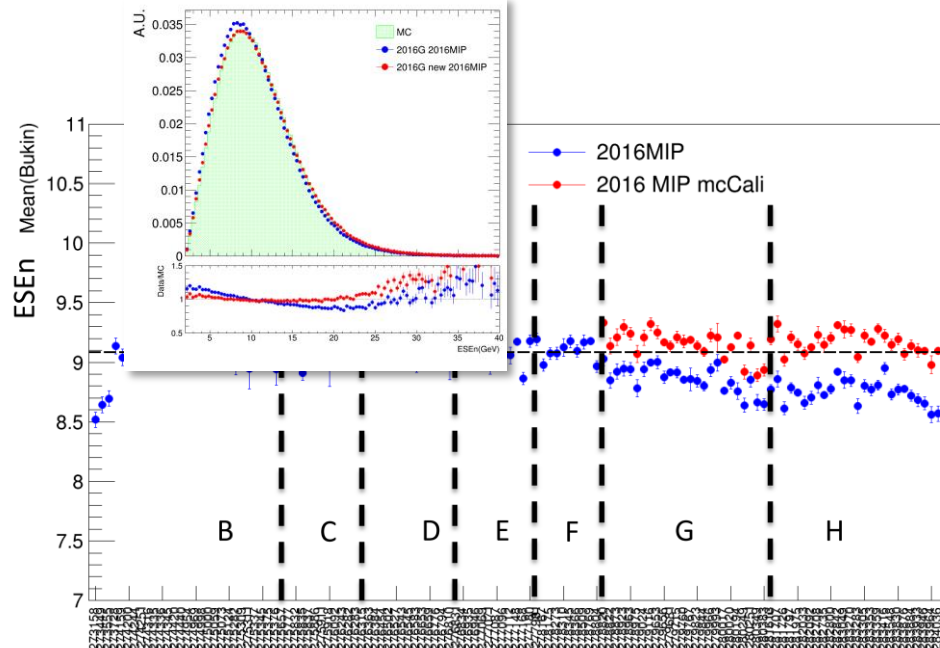




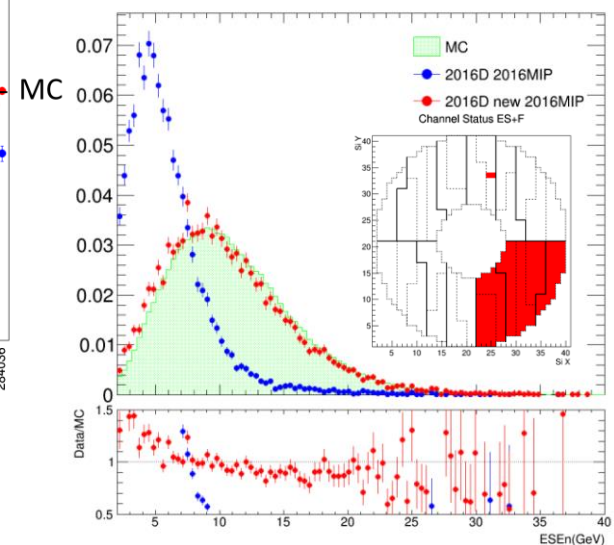
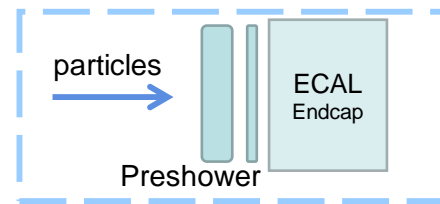
Search for HH production in the $b\bar{b}\gamma\gamma$ final states

Cheng-Wei Yeh (National Central University)

Work for the preshower detector

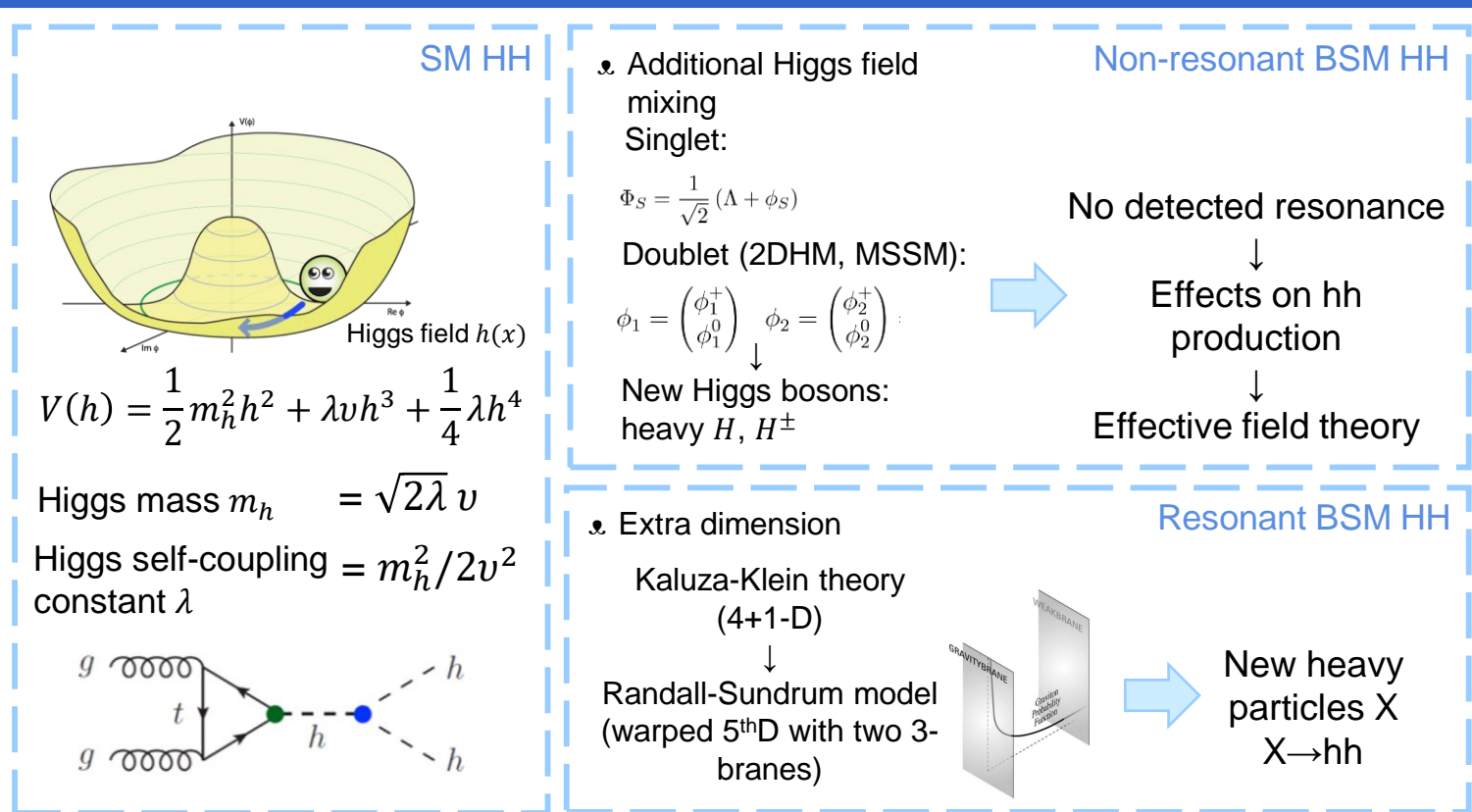


MC/data calibration



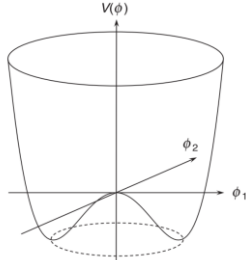
Dead plane calibration 2

Theoretical overview



SM Higgs boson

Higgs potential:



$$V(\phi) = \mu^2 \phi^* \phi + \lambda (\phi^* \phi)^2$$

$$\mathcal{L} = (\partial_\mu \phi)^* (\partial_\mu \phi) - V(\phi)$$

The covariant derivatives in EW gauge invariant:

$$\partial_\mu \rightarrow D_\mu$$

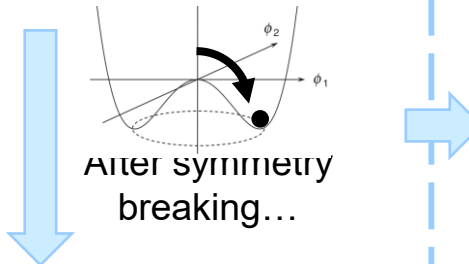
$$= \partial_\mu + i g_W \mathbf{T} \cdot \mathbf{W}_\mu + i g' \frac{Y}{2} B_\mu$$

We obtain:

- $m_W = \frac{1}{2} g_W v$
 - $m_Z = \frac{1}{2} v \sqrt{g_W^2 + g'^2}$
- and also ...
- $m_h = \sqrt{2\lambda} v$
 - $V(h) = \frac{1}{2} m_h^2 h^2 + \lambda v h^3 + \frac{1}{4} \lambda h^4$

Electroweak complex scalar doublet:

$$\phi = \frac{1}{\sqrt{2}} \begin{pmatrix} \phi^+ \\ \phi^0 \end{pmatrix}$$



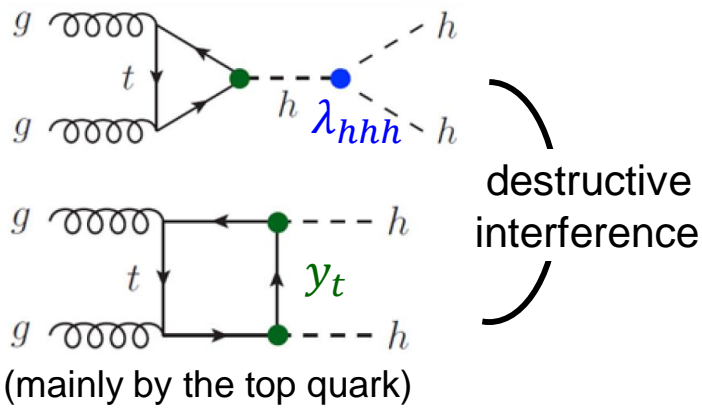
$$\phi = \frac{1}{\sqrt{2}} \begin{pmatrix} 0 \\ v + h(x) \end{pmatrix}$$

$$v \sim 246 \text{ GeV}$$

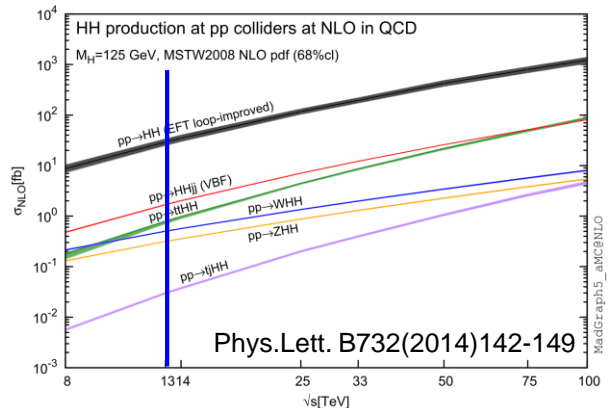
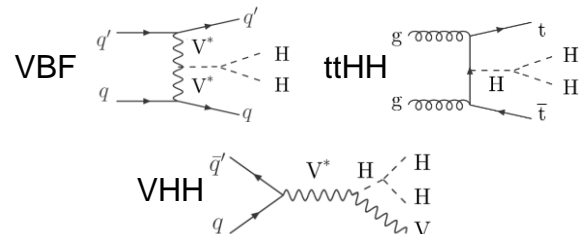
Now we have found the SM-like Higgs boson m_H , we need an independent way to prove it!

Extraction of λ

Most possible:



Other production:



Still not expected to be sensitive at LHC
 $\sigma_{HH}^{SM}(13 \text{ TeV}) = 33.45 \text{ fb}_{[1]}$

Triple Higgs production: $\mathcal{O}(\sigma_{HHH}) \sim 0.1 \text{ fb}$



Beyond the Standard Model ...

- BSMs predict that the new heavy particles decaying into di-Higgs boson:
 - Theories with additional singlet, doublet Higgs fields, ...
 - **Extra dimension model**
- The BSMs can effect the HH production in low energy region.

With an additional singlet Higgs field:

$$\Phi_{\text{SM}} = \begin{pmatrix} 0 \\ \frac{1}{\sqrt{2}}(v + \phi_{\text{SM}}) \end{pmatrix}, \quad \Phi_S = \frac{1}{\sqrt{2}}(\Lambda + \phi_S).$$

$$\mathcal{V} = \mu^2 \Phi_{\text{SM}}^\dagger \Phi_{\text{SM}} + \lambda \left(\Phi_{\text{SM}}^\dagger \Phi_{\text{SM}} \right)^2 + m_S^2 \Phi_S^2 + \rho \Phi_S^4 + \eta \Phi_{\text{SM}}^\dagger \Phi_{\text{SM}} \Phi_S^2.$$

$$h = c_\alpha \phi_{\text{SM}} + s_\alpha \phi_S, \quad H = -s_\alpha \phi_{\text{SM}} + c_\alpha \phi_S$$



$$\frac{\lambda_{hhh}}{\lambda_{hhh}^{\text{SM}}} = \left(c_\alpha^3 - s_\alpha^3 \frac{v}{\Lambda} \right) \simeq \left(1 - \frac{3}{2} s_\alpha^2 \right)$$

[arXiv: 1401.0935](https://arxiv.org/abs/1401.0935)



Effective field theory

- A more general approach can be derived by the effective field theory (EFT) with top-down perspective.

$$\mathcal{L}_{\text{eff}} = \mathcal{L}_{\text{SM}} + \sum_i \frac{c_i^{(5)}}{\Lambda} \mathcal{O}_i^{(5)} + \sum_i \frac{c_i^{(6)}}{\Lambda^2} \mathcal{O}_i^{(6)} + \sum_i \frac{c_i^{(7)}}{\Lambda^3} \mathcal{O}_i^{(7)} + \sum_i \frac{c_i^{(8)}}{\Lambda^4} \mathcal{O}_i^{(8)} + \dots$$

2-D & 4-D 5-D 6-D 7-D 8-D

Λ : the mass order with new heavy particles in BSMs

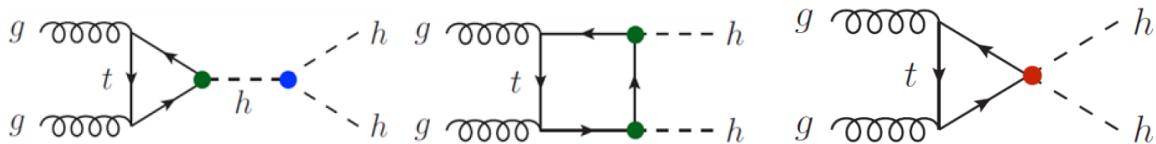
\mathcal{O} : the n-D operator

- The 6-D EFT is focused because 5-D operator violates the lepton number and higher dimensional operators are highly suppressed.[1]

Anomalous coupling

- The 6-D EFT relative to di-Higgs production is rewritten with five anomalous Higgs couplings to provide physics interpretation.

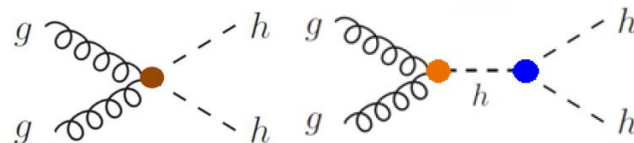
$$\Delta\mathcal{L} = -\underline{\kappa_\lambda}\lambda_{SM}vH^3 - \frac{m_t}{v}\left(v + \underline{\kappa_t}H + \frac{c_2}{v}H^2\right)(\bar{t}_L t_R + h.c.) + \frac{1}{4}\frac{\alpha_s}{3\pi v}\left(c_gH - \frac{c_{2g}}{2v}H^2\right)G^{\mu\nu}G_{\mu\nu}, \text{ where } \underline{\kappa_\lambda} = \lambda_{HHH}/\lambda_{HHH}^{SM}, \underline{\kappa_t} = y_t/y_t^{SM}$$



Tri-linear coupling

Yukawa interaction

ttHH interaction



Higgs-gluon contact interactions

Anomalous coupling

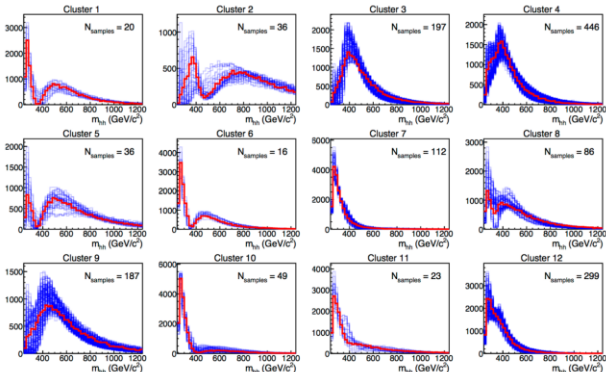
- Effect on the cross section of the di-Higgs production:

$$\begin{aligned} \frac{\sigma_{HH}}{\sigma_{HH}^{SM}} = & A_1 \kappa_t^4 + A_2 c_2^2 + (A_3 k_t^2 + A_4 c_g^2) \kappa_\lambda^2 + A_5 c_{2g}^2 \\ & + (A_6 c_2 + A_7 \kappa_t \kappa_\lambda) \kappa_t^2 + (A_8 \kappa_t \kappa_\lambda + A_9 c_g \kappa_\lambda) c_2 \\ & + A_{10} c_2 c_{2g} + (A_{11} c_g \kappa_\lambda + A_{12} c_{2g}) \kappa_t^2 \\ & + (A_{13} \kappa_\lambda c_g + A_{14} c_{2g}) \kappa_t \kappa_\lambda + A_{15} c_g c_{2g} \kappa_\lambda. \end{aligned}$$



The coefficient A_i is extracted by MC simulation.

- Effect on the kinematics m_{HH} , $\cos\theta_{HH}$:



- The benchmark points are defined according to the shapes of kinematics.
- Rely on the **kinematics reweighting technique** to approach the full 5-D space of the coupling constants!

BSM resonance HH

- Warped extra dimension theory (WED):
 - Extra dimension (5-D) theory by Kaluza and Klein (KK theory)
 - Randall and Sundrum (RS) model
- Warped 5-D metric :

$$ds^2 = e^{-2kr_c\phi} \eta_{\mu\nu} dx^\mu dx^\nu + r_c^2 d\phi^2$$

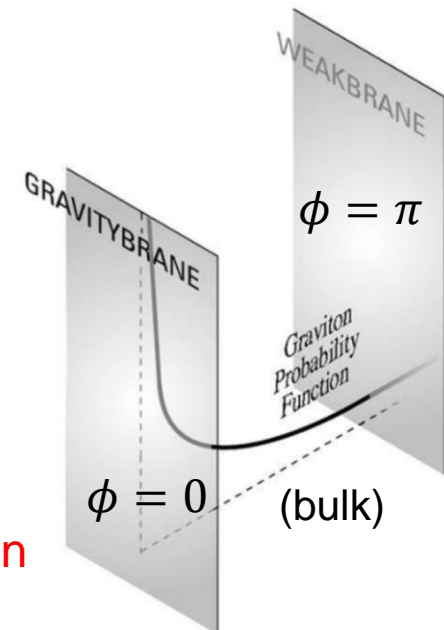
Warped factor 4-D metric 5th D and radius

New particles come from the fluctuation of the metric:

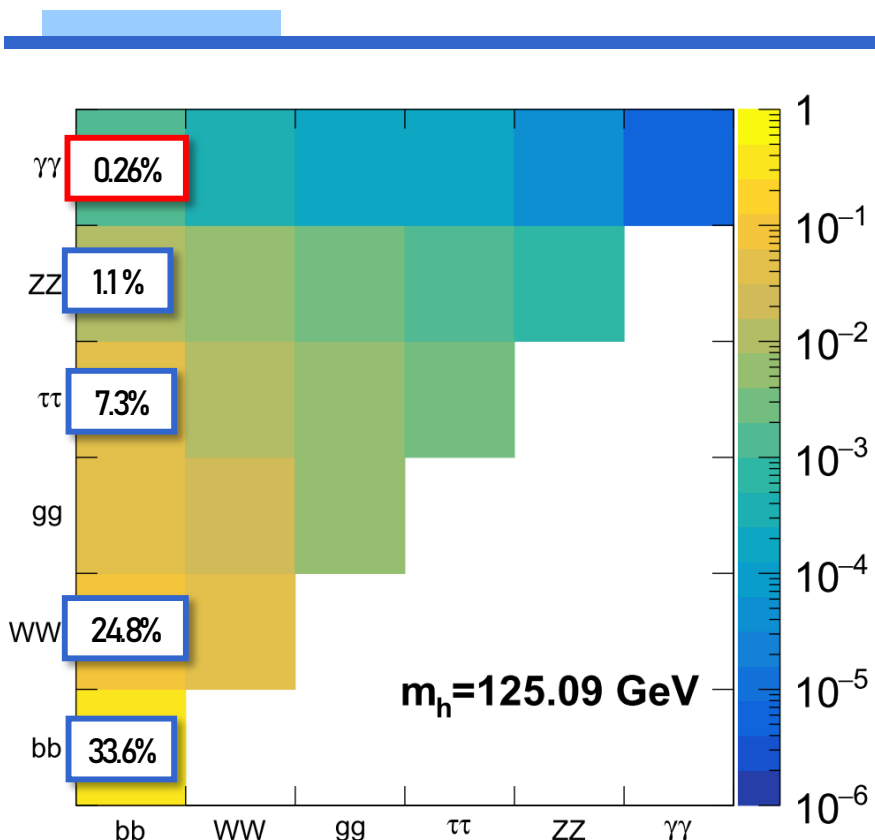
$$\delta g_{MN}(x, \phi) = \begin{pmatrix} h_{\mu\nu}(x, \phi) & | & h_{\mu,5}(x, \phi) \\ \hline | & & | \\ h_{\mu,5}(x, \phi) & & h_{55}(x, \phi) \end{pmatrix}$$

Spin-2 graviton

Spin-0 radion



Final state



- $bbbb$: largest BR, large QCD and $t\bar{t}$ background
- $bbWW$: large BR and $t\bar{t}$ background
- $bb\tau\tau$: sizeable BR, relatively small background
- $bb\gamma\gamma$: small BR, full reconstructed, good resolution of $\gamma\gamma$, small background



Dataset

Data:

- Collision energy $\sqrt{s} = 13$ TeV from the LHC
- Recorded by the CMS in 2016, 35.9 fb^{-1}
- Pass di-photon high level trigger.

Background:

- $n\gamma + \text{jets}$ events from QCD, estimated by the selected data.
- Simulated single-Higgs production background for the non-resonant search.

Signal Monte Carlo samples:

- $gg \rightarrow X \rightarrow HH \rightarrow bb\gamma\gamma$, X mass from 250 to 900 GeV with spin-0 and spin-2.
- $gg \rightarrow HH \rightarrow bb\gamma\gamma$ with benchmark coupling constants.

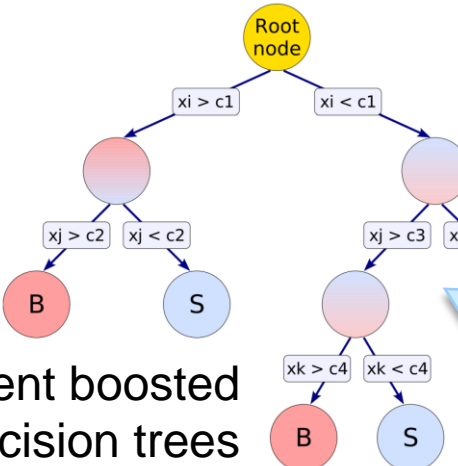


Event selection

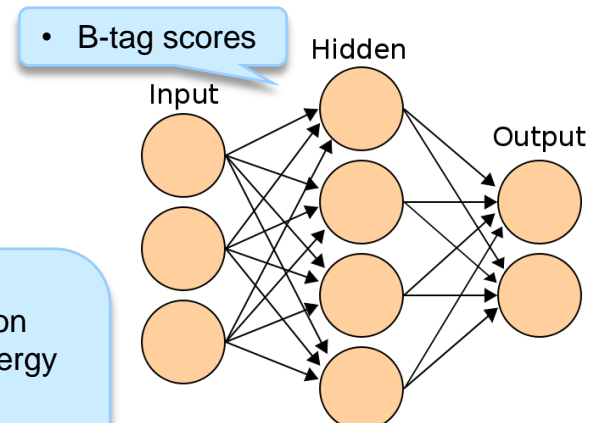
- Photon selection:
 - Trigger mimic pre-selection, photon MVA identification
 - $E_T(\gamma_1) > 30 \text{ GeV}$, $E_T(\gamma_2) > 20 \text{ GeV}$, $|\eta| < 2.5$ and excludes the gap of ECAL
 - $E_T(\gamma_1)/M_{\gamma\gamma} > 1/3$, $E_T(\gamma_2)/M_{\gamma\gamma} > 1/4$
 - $100 < M_{\gamma\gamma} < 180 \text{ GeV}$
- Jet selection:
 - Loose jet identification
 - $\Delta R(Jet, \gamma) > 0.4$
 - $p_T > 25 \text{ GeV}$, $|\eta| < 2.4$
 - $70 < M_{jj} < 190 \text{ GeV}$
 - Select the pair with the highest sum of b-tag scores

Multivariate analysis (MVA)

- Many variables (features) help us to select the signal or correct the observables.
- To combine all of information, we rely on the multivariate analysis (MVA).

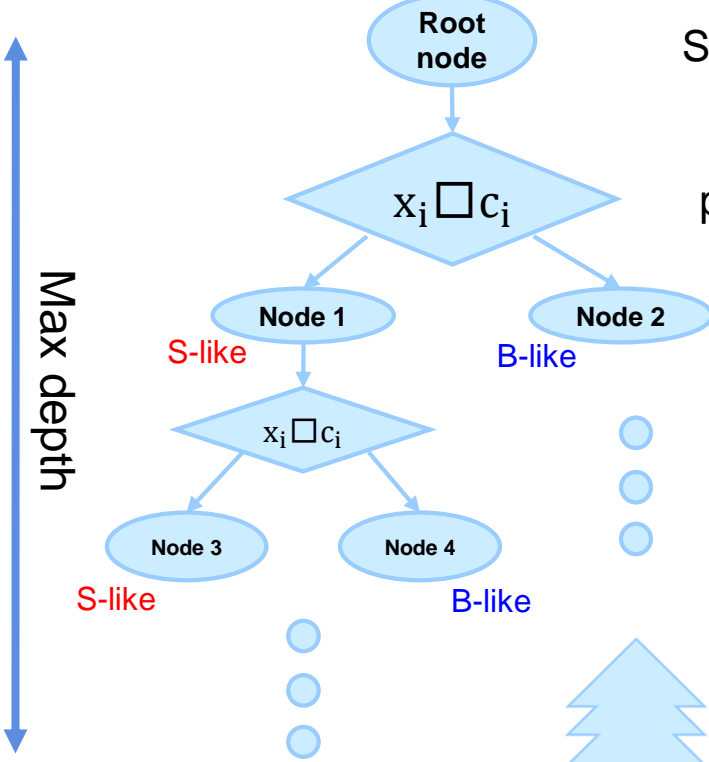


- Photon identification
- Photon energy regression
- **B-jet energy regression**
- Event categorization

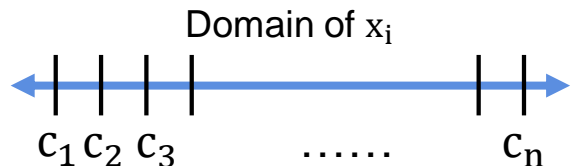




Decision trees



Scan the provided variables x_i
and cut value c_i
Get the best separation
power/average square error.



Then we get a tree ...



Gradient boost



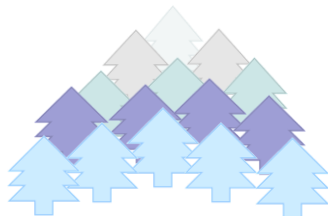
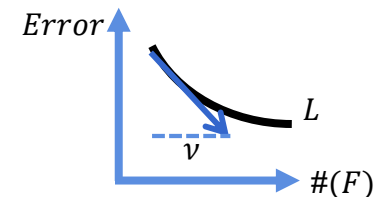
A small tree (weak learner) has bad prediction $F(\mathbf{x})$.
The error rate of a tree can be described
by “Loss Function” = $L(F(\mathbf{x}), y)$.

(\mathbf{x} is the vector of the input variables, y is the target value we want to predict.)



Another tree can be grown and try to predict $F(\mathbf{x}) + v h(\mathbf{x})$,
where $h(\mathbf{x}) = -\frac{\partial L(F(\mathbf{x}), y)}{\partial F(\mathbf{x})}$. (like gradient descend)

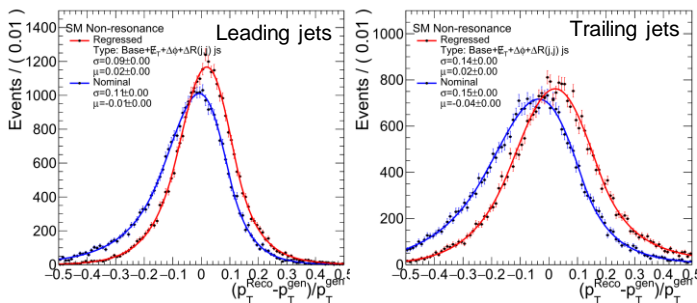
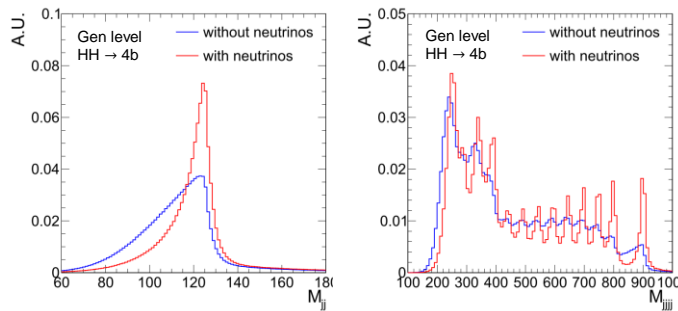
We plant more and more trees.



Then we get a forest with a good prediction power!

B-jet energy regression

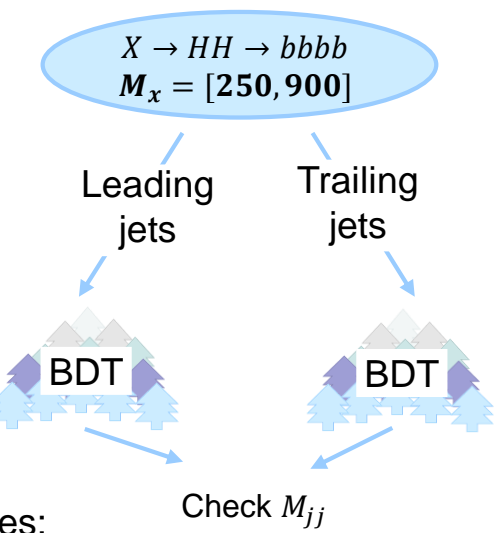
The specific b-jet energy regression is trained by BDT to predict the correct energy of b-jets.



2018/6/22

Gen-matched jets:

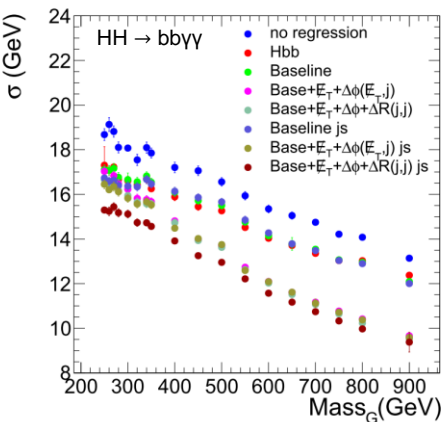
- $p_T > 20 \text{ GeV}$
- $|\eta| < 2.4$
- include the neutrinos within $\Delta R < 0.4$.



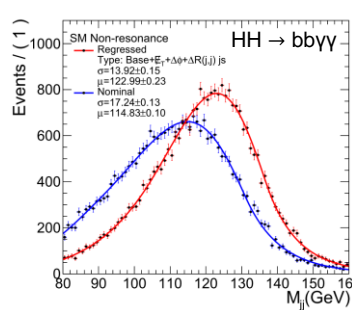
Training variables:

- 15 variables based on jet's constituents and secondary vertex information
- Additional 3 variables: **MET**, $\Delta\phi(j, \text{MET})$ and ΔR between two jets

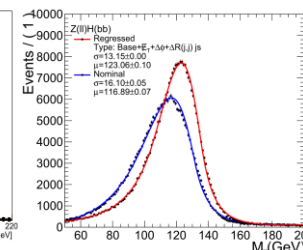
Regression improvement



The improvement from the 3 additional variables and the training strategy is checked.



- M_{jj} resolution is improved by ~18% (depending on kinematic region)
- M_{jj} scale is closer to 125 GeV.



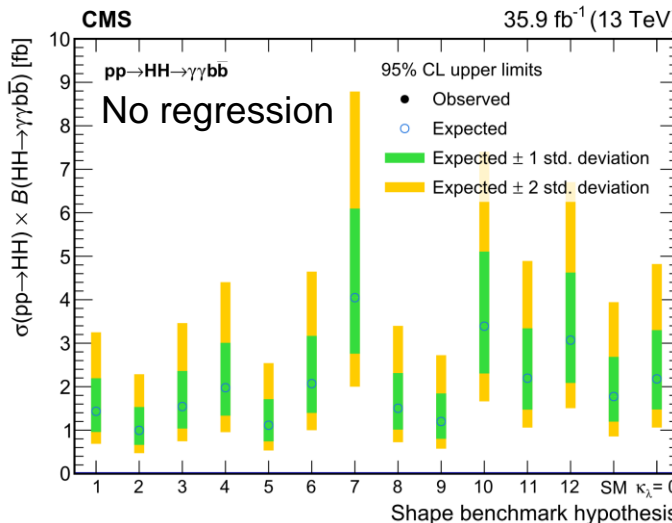
Resolution improvement in $Z(\text{II})H(\text{bb})$:
8% (old regression)
↓
18% (new regression)

Regression improvement

In SM-like HH search:

- S/B ratios are improved 4 ~ 20% (depending on the different categories)
- Expected upper limits on cross section: $1.77 \text{ fb} \rightarrow 1.6 \text{ fb}$

Impact on non-resonant benchmark search:

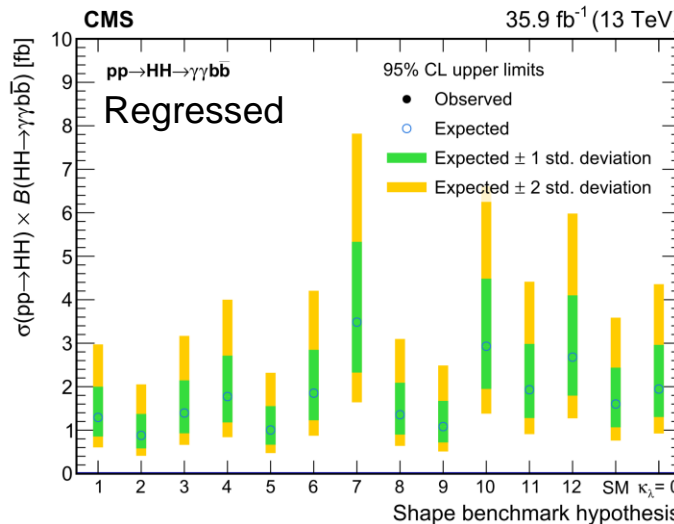


Regression improvement

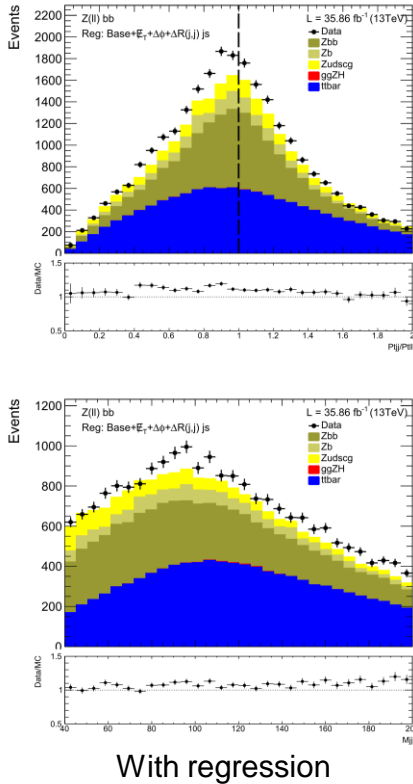
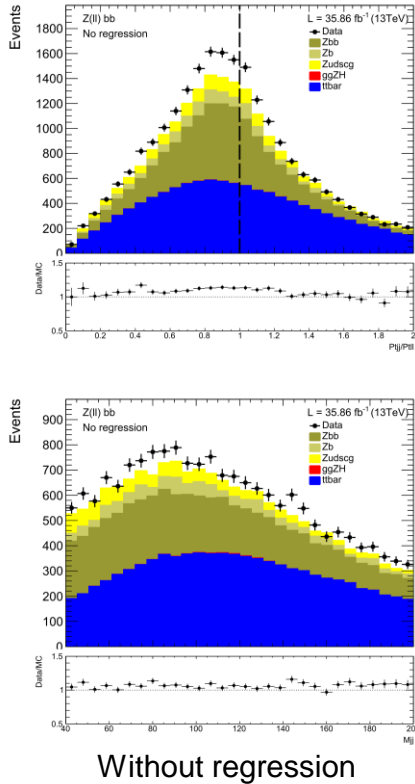
In SM-like HH search:

- S/B ratios are improved 4 ~ 20% (depending on the different categories)
- Expected upper limits on cross section: $1.77 \text{ fb} \rightarrow 1.6 \text{ fb}$

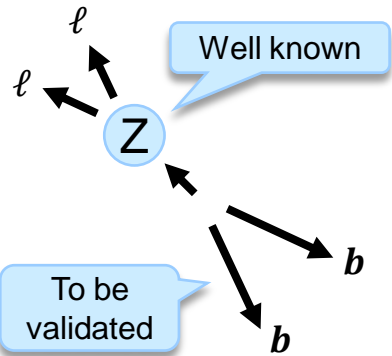
Impact on non-resonant benchmark search:



Regression validation



- Validated by:

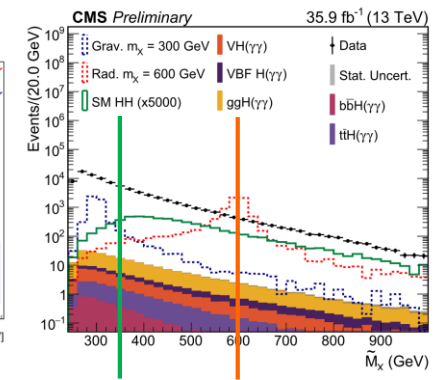
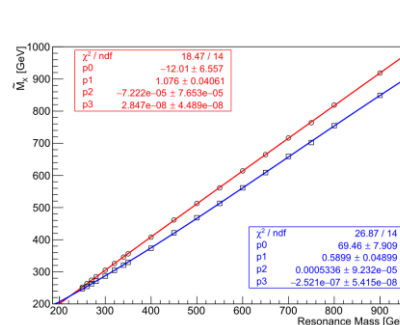
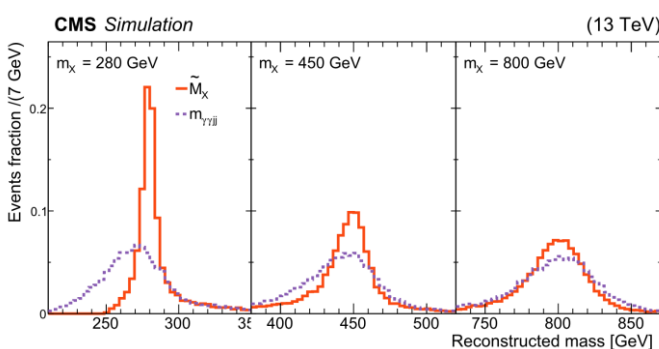


- p_T balance between $Z(II)$ and bb ($p_{T,jj}/p_{T,ll}$) scale is closer to one.
- There is no significant distortion in M_{jj} shape after regression.

Effective mass \tilde{M}_X

To optimize the mass window cut, the effective mass is defined as:

$$\tilde{M}_X = M_{jj\gamma\gamma} - M_{jj} - M_{\gamma\gamma} + 250 \text{ (GeV)}$$



Minimize the dependency on the jet/photon energy resolution and scale.

Resonant mass window covers 60% of signal shape in M_X around peak.

Two defined \tilde{M}_X regions:
 Resonance: 600 GeV
 Non-Resonance: 350 GeV

Categorization MVA

Training samples:

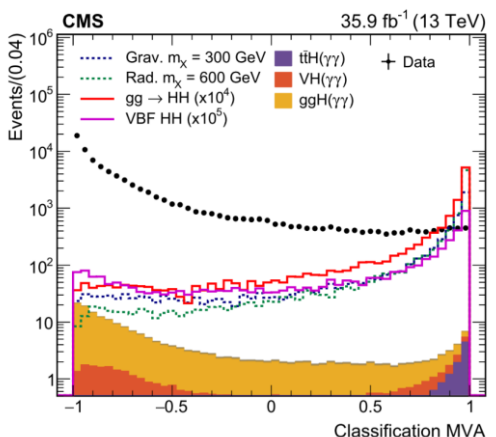
- Signal: Resonant and non-resonant signal samples, trained separately.
- Background: **photon control region** of data (at least one photon failed ID)

Training variables:

- b-tag scores of two jets, $p_T(\gamma\gamma)/M_{jj\gamma\gamma}$, $p_T(jj)/M_{jj\gamma\gamma}$
- The angles between selected objects

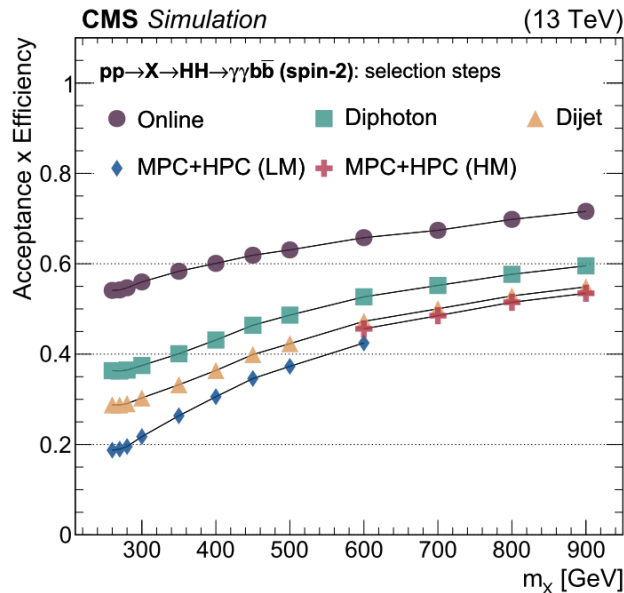
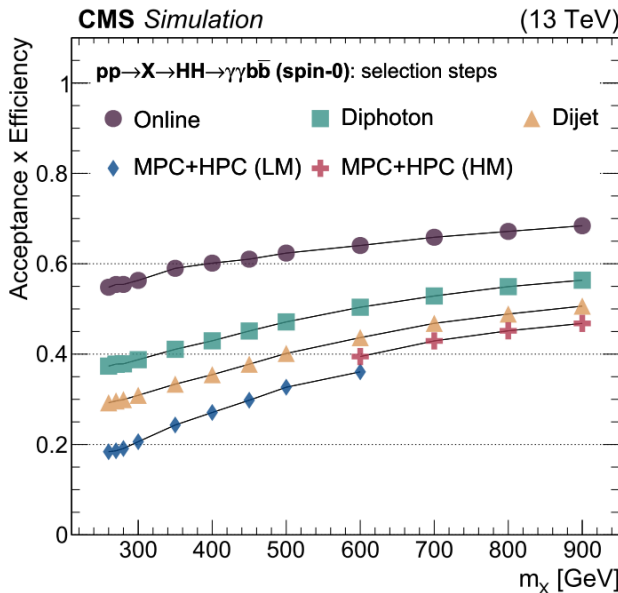
HPC: High Purity Category
MPC: Medium Purity Category

	M _x	MVA Categorization
Non-Resonant	M _x > 350	HPC: MVA > 0.97 MPC: 0.6 < MVA < 0.97
	M _x < 350	HPC: MVA > 0.985 MPC: 0.6 < MVA < 0.985
Resonant	M _x > 600	HPC: MVA > 0.5 MPC: 0 < MVA < 0.5
	M _x < 600	HPC: MVA > 0.96 MPC: 0.7 < MVA < 0.96



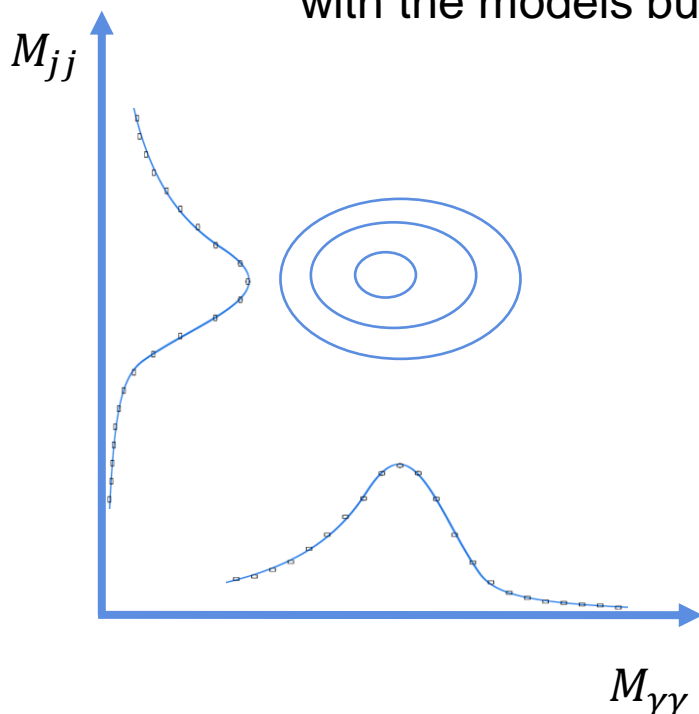
Optimized cut values

Signal efficiency



- Resonant HH efficiency: 20% ~ 50%, which is mass dependent.
- SM HH efficiency: ~30% in sum of all categories.

Modeling strategy



To estimate the signal strength, the data are compared with the models built by $M_{\gamma\gamma}$ and M_{jj} distribution.

Signal model:

- Simulated samples fit by peaking function

Background model:

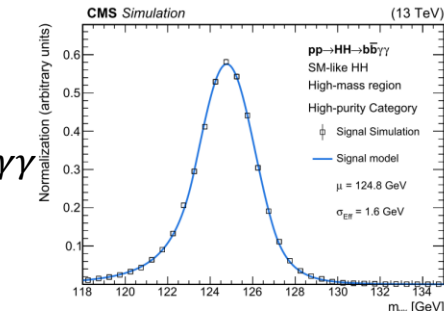
- Selected data fit by smooth falling function

The 2-D fit is performed for $M_{\gamma\gamma}$ and M_{jj} with the product of two independent function.

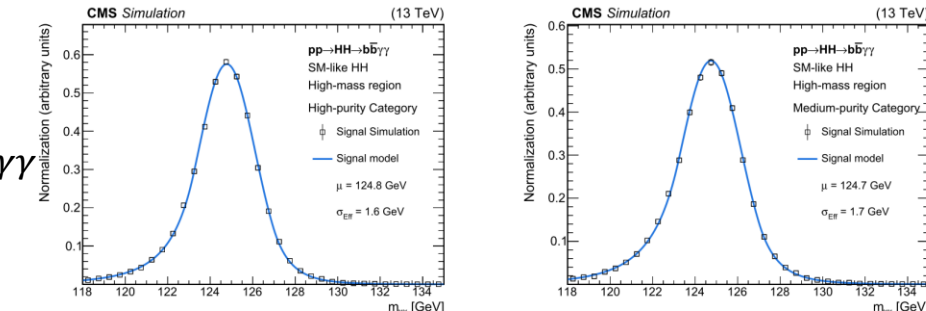


Signal modeling

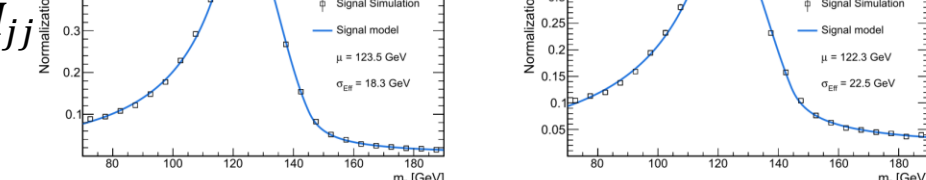
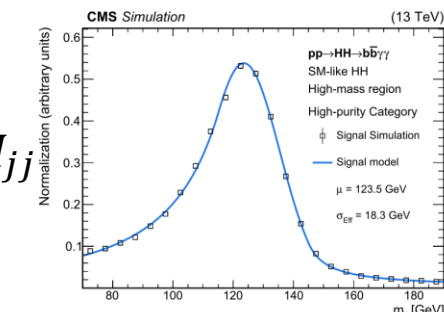
HPC



MPC



M_{jj}



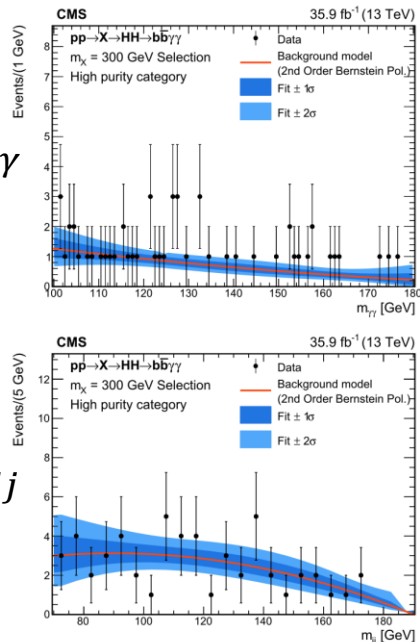
SM HH, High mass region

- Fit by **double-sided crystal ball functions (DSCB)**: DSCB (M_{jj}) \times DSCB ($M_{\gamma\gamma}$)
- Uncorrelation hypothesis is checked.

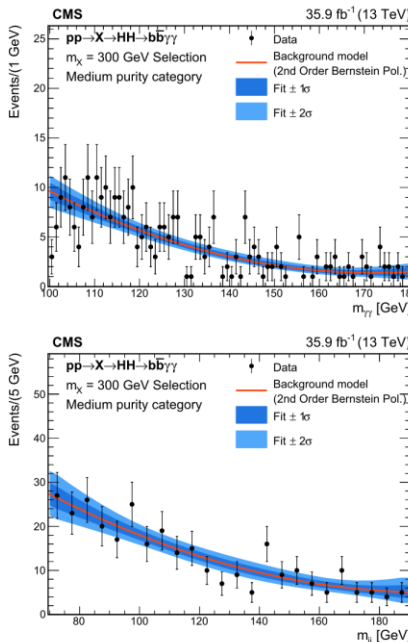


Background modeling (resonant)

HPC



MPC

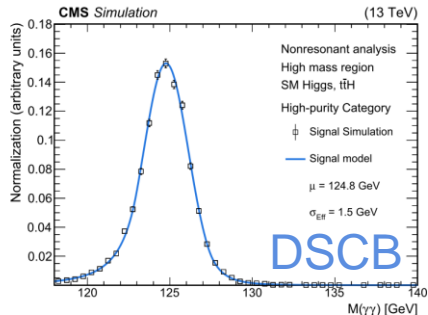


- Fit by **Bernstein Polynomials**:
 - #Events <15: 1st order
 - #Events >15: 2nd order
- They are found unbiased with respect to other possible fit functions.
- Uncorrelation hypothesis is found valid.

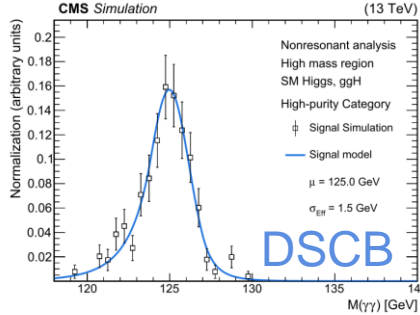
Resonant HH, $\tilde{M}_X = 300$ (GeV)

Single Higgs background modeling

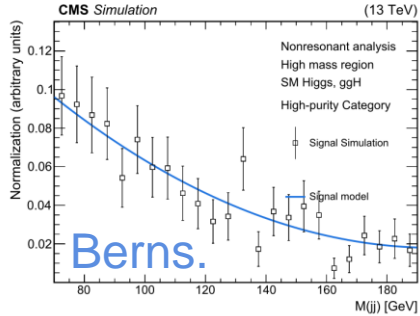
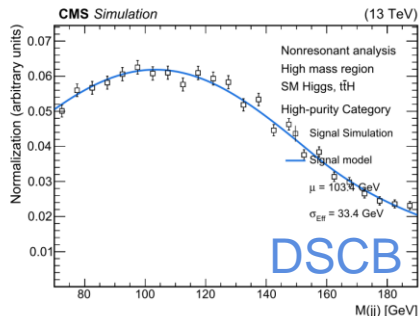
ttH



ggH



M_{jj}



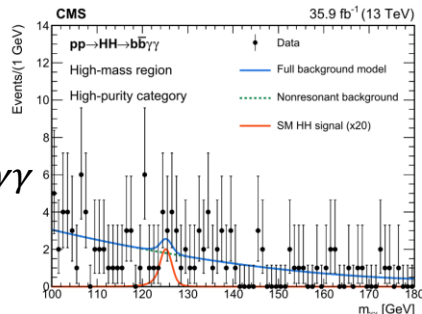
SM single Higgs, High Mass High Purity

- Higgs background contamination in the non-resonant search is non-negligible.
- Accounted production: ggH, VBF, VH, ttH and bbH.
- Fit function:
DSCB (M_{jj}) \times DSCB ($M_{\gamma\gamma}$)
for VH, ttH, bbH

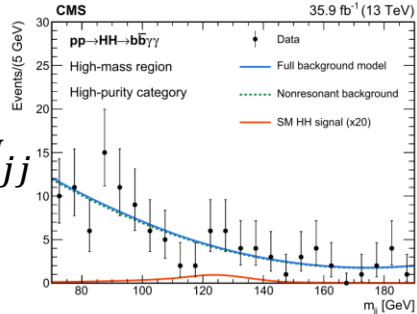
Berns. (M_{jj}) \times DSCB ($M_{\gamma\gamma}$)
for ggH, VBF

Background modeling (non-resonant)

HPC

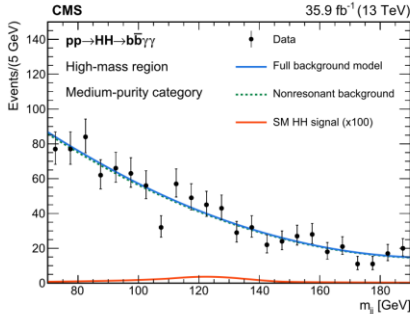
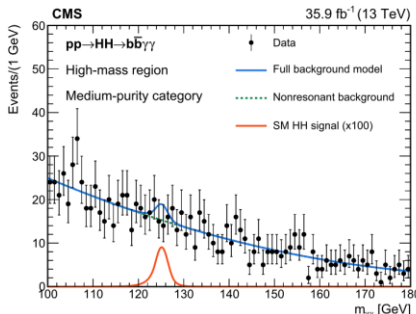


$M_{\gamma\gamma}$



SM HH, High mass region

MPC



- The fit function is chosen as the same for the resonance study.
- The full background modeling includes the fixed single-Higgs constituent and compared to the signal shape.



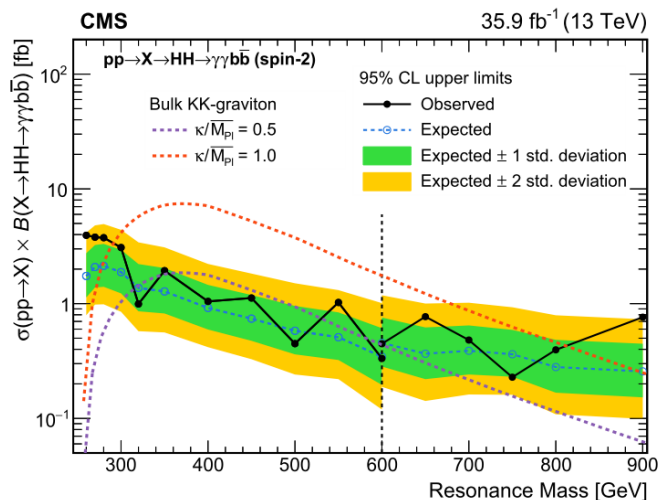
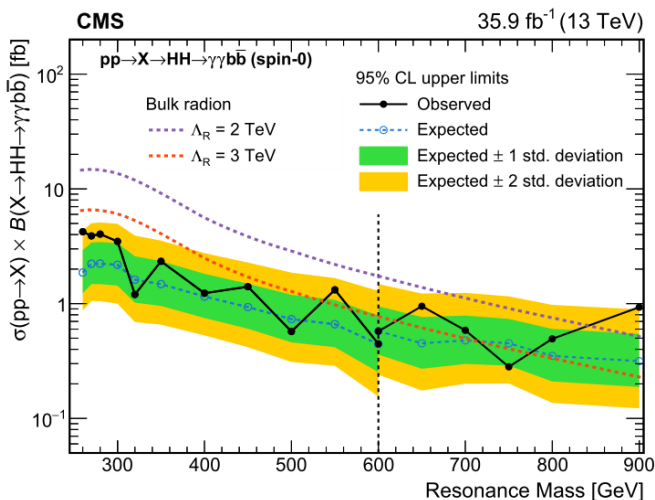
Systematic uncertainties

Source of systematic uncertainties	Type	Value
General uncertainties		
Integrated luminosity	Normalization	2.5%
Photon related uncertainties		
PES $\frac{\Delta M_{\gamma\gamma}}{M_{\gamma\gamma}}$	Shape	2.0%
PER $\frac{\Delta \sigma M_{\gamma\gamma}}{\sigma M_{\gamma\gamma}}$	Shape	1.0%
Di-photon selection (with trigger uncertainties and PES)	Normalization	0.5%
Photon identification	Normalization	5.0%
Jet related uncertainties		
JES $\frac{\Delta M_{jj}}{M_{jj}}$	Shape	0.5%
JER $\frac{\Delta \sigma M_{jj}}{\sigma M_{jj}}$	Shape	1.0%
Di-jet selection (JES+JER)	Normalization	5.0%
Resonant analysis specific uncertainties		
Mass window selection (JES+JER)	Normalization	3.0%
Classification MVA (HPC)	Normalization	11-19%
Classification MVA (MPC)	Normalization	3-9%
Non-resonant analysis specific uncertainties		
M_x Classification	Normalization	0.5%
Classification MVA (HPC)	Normalization	11-19%
Classification MVA (MPC)	Normalization	3-9%
Theoretical uncertainties of SM single-Higgs boson production		
QCD missing orders (ggH, VBF H, VH, ttH)	Normalization	0.4-5.8%
PDF and uncertainties (ggH, VBF H, VH, ttH)	Normalization	1.6-3.6%
Theory uncertainty bbH	Normalization	20%
Theoretical uncertainties of SM di-Higgs boson production		
QCD missing orders	Normalization	4.3-6%
PDF and α_s uncertainties	Normalization	3.1%
m_T effects	Normalization	5%

- Shape uncertainties act upon the shapes of our modeling.
- Normalization uncertainties act upon the expected yields.
- Theory uncertainties are also applied according to the recommendations from LHC Higgs cross section working group. [1]



Resonant HH result



Excluded range:

Spin-0 Radion

$$\Lambda_R = 3 \text{ TeV}: \quad M_R < 540 \text{ GeV}$$

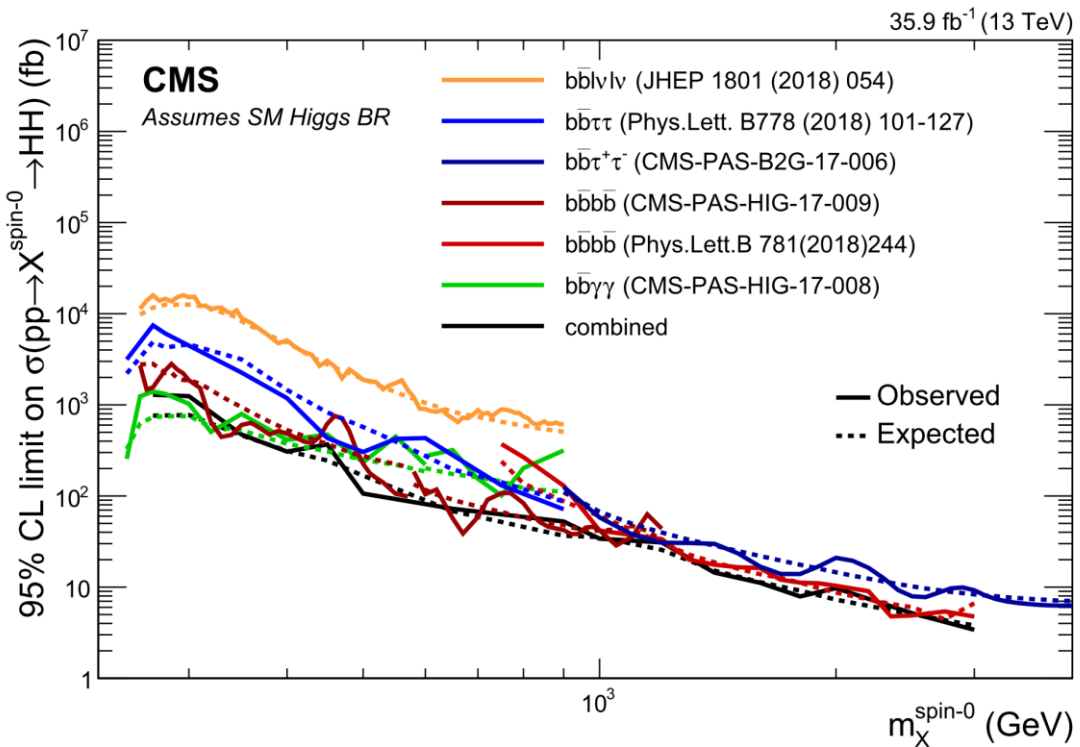
$$\Lambda_R = 2 \text{ TeV}: \quad M_R < 840 \text{ GeV}$$

Spin-2 Graviton

$$\kappa/\overline{M_{pl}} = 0.5: \quad 350 < M_R < 530 \text{ GeV}$$

$$\kappa/\overline{M_{pl}} = 1.0: \quad 290 < M_R < 810 \text{ GeV}$$

Resonant HH common plots



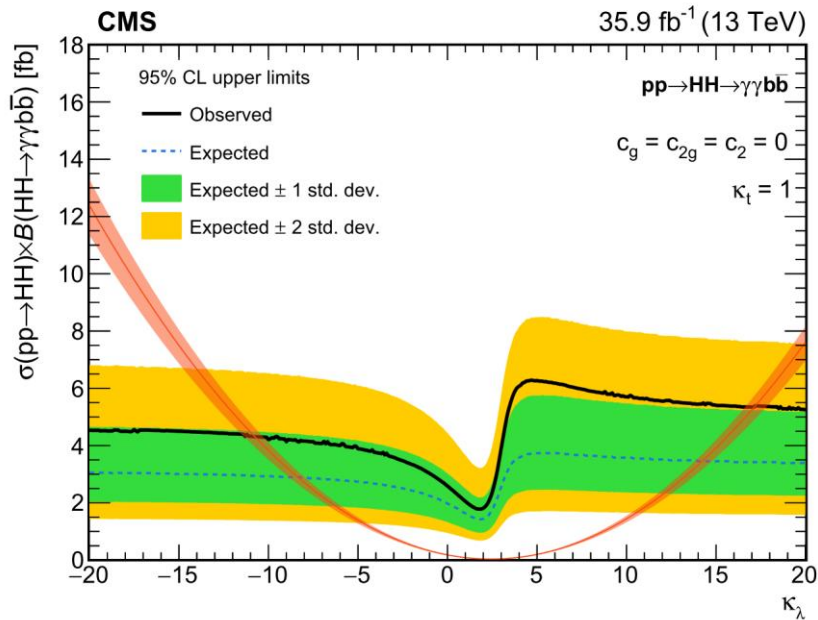
HH $\rightarrow b\bar{b}\gamma\gamma$ leads the best sensitivity at the low mass region.



SM HH result

- Limits in each categories of SM HH are combined.
- Expected limit on:
 - $\sigma(pp \rightarrow HH) \times \text{Br}(HH \rightarrow bb\gamma\gamma) = 1.6 \text{ fb}$
 - $\sigma(pp \rightarrow HH) = 0.63 \text{ pb} (19 \times \text{SM})$
- Observed limit on:
 - $\sigma(pp \rightarrow HH) \times \text{Br}(HH \rightarrow bb\gamma\gamma) = 2.0 \text{ fb}$
 - $\sigma(pp \rightarrow HH) = 0.79 \text{ pb} (24 \times \text{SM})$

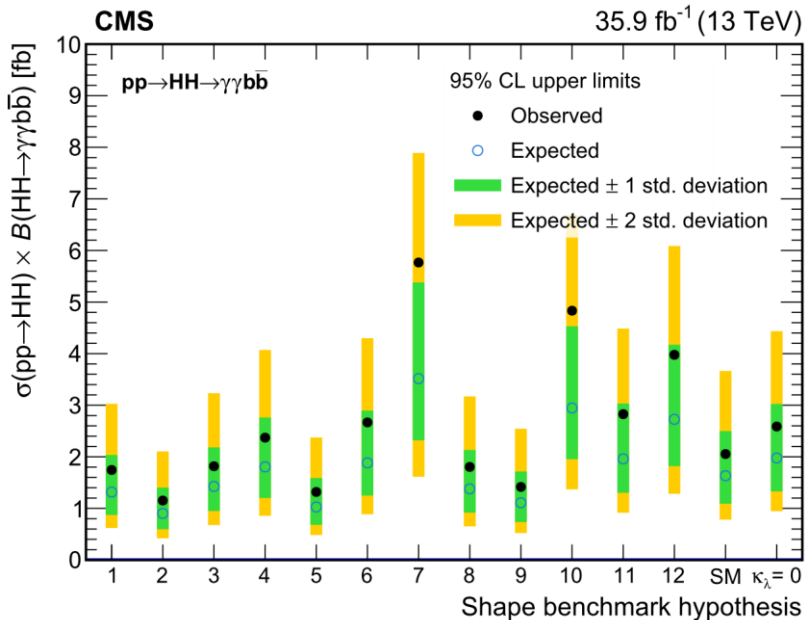
BSM non-resonant HH result



The limits of k_λ scanning exclude $k_\lambda < -11$ and $k_\lambda > 17$ region.



BSM non-resonant HH result



No statistically significant deviations are found.



Summary

- All observed results are consistent with expected prediction.
No significant excess is observed.
- The exclusion are performed on the resonant HH hypotheses
and the modified Higgs coupling hypotheses.
- Expected limits are set on the SM-like HH production in $b\bar{b}\gamma\gamma$
channel at 1.6 fb ($19 \times$ SM).
 - Run I (8TeV, 19.7 fb^{-1}): 1.56 fb ($62 \times$ SM) [1]
 - 2015 Run II (13TeV, 2.7 fb^{-1}): 7.85 fb ($90 \times$ SM) [2]
- The result has been submitted to Phys. Lett. B. [3]



Thanks for the attention!



BACK UP



Non-resonance benchmarks points

Benchmark	κ_λ	κ_t	c_2	c_g	c_{2g}
1	7.5	1.0	-1.0	0.0	0.0
2	1.0	1.0	0.5	-0.8	0.6
3	1.0	1.0	-1.5	0.0	-0.8
4	-3.5	1.5	-3.0	0.0	0.0
5	1.0	1.0	0.0	0.8	-1
6	2.4	1.0	0.0	0.2	-0.2
7	5.0	1.0	0.0	0.2	-0.2
8	15.0	1.0	0.0	-1	1
9	1.0	1.0	1.0	-0.6	0.6
10	10.0	1.5	-1.0	0.0	0.0
11	2.4	1.0	0.0	1	-1
12	15.0	1.0	1.0	0.0	0.0
SM	1.0	1.0	0.0	0.0	0.0

[10.1007/JHEP04\(2016\)126](https://doi.org/10.1007/JHEP04(2016)126)

Reweighting

$$\begin{aligned} \frac{\sigma_{HH}}{\sigma_{SM}^{SM}} = & A_1 \kappa_t^4 + A_2 c_2^2 + (A_3 k_t^2 + A_4 c_g^2) \kappa_\lambda^2 + A_5 c_{2g}^2 \\ & + (A_6 c_2 + A_7 \kappa_t \kappa_\lambda) \kappa_t^2 + (A_8 \kappa_t \kappa_\lambda + A_9 c_g \kappa_\lambda) c_2 \\ & + A_{10} c_2 c_{2g} + (A_{11} c_g \kappa_\lambda + A_{12} c_{2g}) \kappa_t^2 \\ & + (A_{13} \kappa_\lambda c_g + A_{14} c_{2g}) \kappa_t \kappa_\lambda + A_{15} c_g c_{2g} \kappa_\lambda. \end{aligned}$$

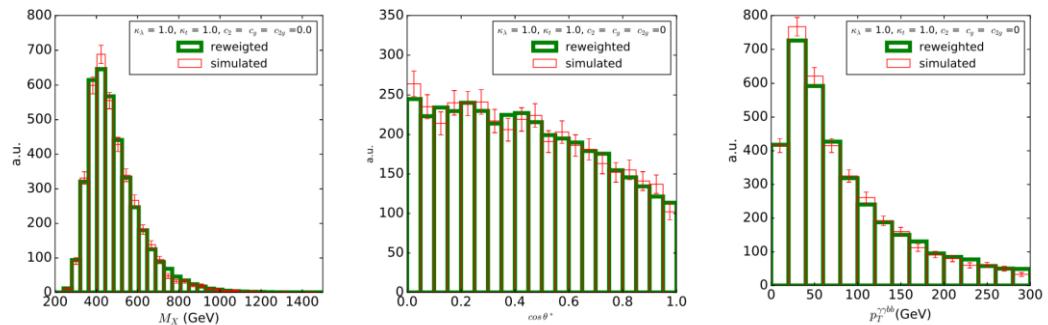


The differential cross-section in m_{hh} , $\cos\theta$:

$$R_{HH}^j = \frac{\sigma_{HH}}{\sigma_{HH}^{SM}} \frac{Frac_{SM}^j}{Frac_{SM}^j} = Poly(A_i^j)$$

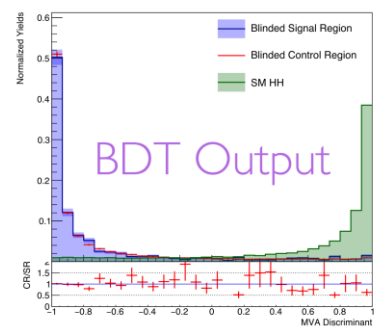
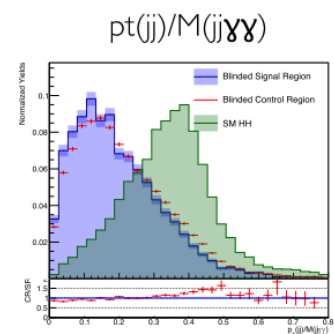
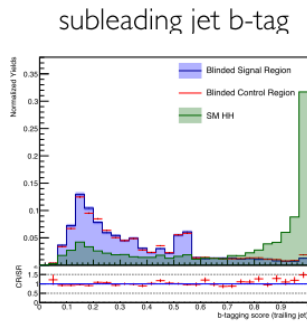
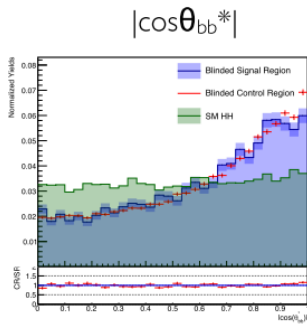
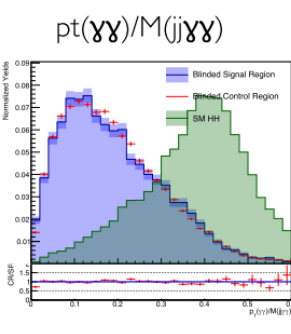
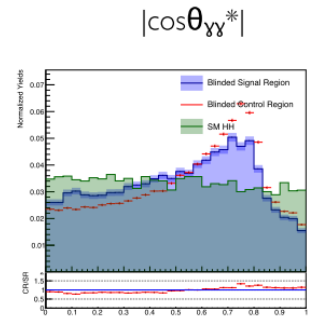
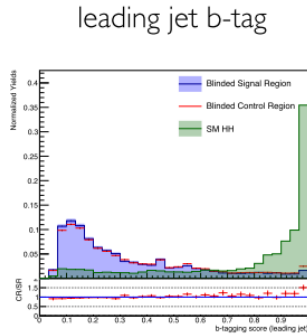
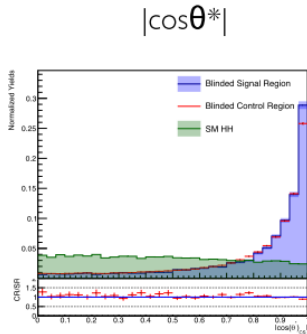
Weight:

$$W_j = R_{HH}^j \frac{\sigma_{HH}^{SM}}{\sigma_{HH}} \frac{Frac_{SM}^j}{C_{norm}}$$





Categorization MVA variables





B-jet regression variables

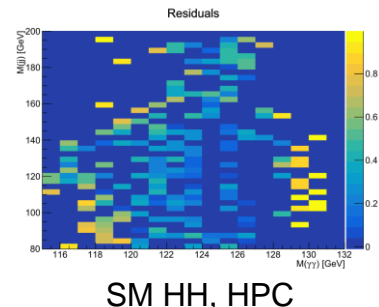
Input variables as in $H \rightarrow b\bar{b}$ analysis	
nPVs	Number of primary vertex of the event
Jet p_T	Jet transverse momentum
Jet η	Jet pseudorapidity
Jet m_T	Jet transverse mass
Jet lead track p_T	Transverse momentum of the leading track in the jet
Jet lepton p_T	Transverse momentum of the leading lepton candidate in the jet
Jet relative lepton p_T	The projection of 4-momentum of the leading lepton candidate in the jet on the jet axis.
ΔR (Jet, lepton)	The distance in the η - ϕ space of the lepton in the jet and the jet
Jet neHEF	Neutral hadron energy fraction of the jet
Jet neEmF	Photon energy fraction of the jet
Jet vtx p_T	p_T of the jet secondary vertex
Jet vtx Mass	Invariant mass of the jet secondary vertex
Jet vtx 3d L	The 3-d flight length of the jet secondary vertex
Jet vtx Ntrk	Track multiplicity of the reconstructed secondary vertex
Jet vtx 3d eL	Error on the 3-d flight length of the jet secondary vertex
Additional variables for this analysis	
MET	Missing energy of the event
$\Delta\phi(Jet, MET)$	The difference ϕ of MET and the jet
$\Delta R(Jet_1, Jet_2)$	The distance in the η - ϕ space of two jets

Correlation study

For signal model:

- Check the difference between MC sample and models.

$$R_{ij} = \frac{N_{ij}^{\text{PDF}} - N_{ij}^{\text{MC}}}{\sigma_{N_{ij}^{\text{PDF}}}^{\text{Poisson}}}$$

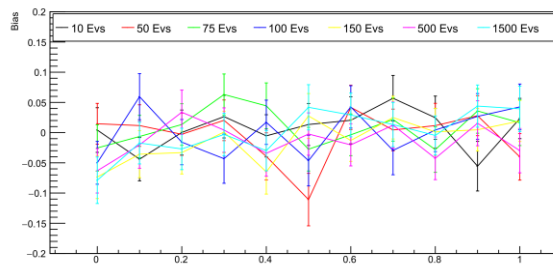


For background model:

- Check missing degree of freedom.
Generate several toys by:

$$g_{\text{corr}}(x, y) = g(x, y) + [\alpha \cdot m_{\gamma\gamma} \cdot m_{jj} + \beta \cdot m_{\gamma\gamma}^2 \cdot m_{jj} + \omega \cdot m_{\gamma\gamma} \cdot m_{jj}^2]$$

Fit by the chosen function and check the bias.



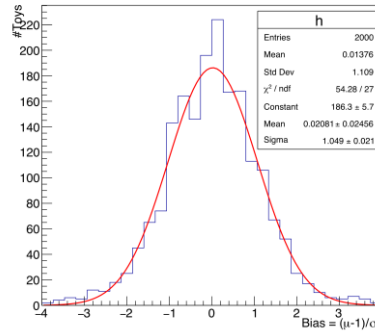
Bias study

- Fit the data in photon control region by the other candidates for background modeling.
 - Candidate functions:
Laurent series, sums of n exponential functions
- Generate several toys injected the signal and fit it by the chosen function and check the bias:

$$(\mu_{fit} - \mu_{true})/\sigma_\mu$$

where signal strength μ is the

$$F = \mu \cdot Signal + Background$$



	E _T																		
	L4L4	L3L3	L2L2	L1L1	B4B4	B3B3	B2B2	B1B1	B1B1	B2B2	B3B3	B4B4	L1L1	L2L2	L3L3	L4L4	E1E1	E2E2	E3E3
#	0.12 ± 0.09	0.09 ± 0.04	0.07 ± 0.04	0.03 ± 0.04	0.01 ± 0.04	0.02 ± 0.05	0.03 ± 0.04	0.03 ± 0.04	0.10 ± 0.04	0.07 ± 0.04	0.06 ± 0.04	0.09 ± 0.04	0.03 ± 0.04	0.04 ± 0.04	0.06 ± 0.04	0.10 ± 0.04			
Mean	0.01376	-0.01	-0.02	-0.01	0.02	0.01	0.02	0.01	0.01	0.01	0.01	0.01	0.01	0.01	0.01	0.01	0.01	0.01	
Std Dev	1.109	1.15	1.15	1.15	1.15	1.15	1.15	1.15	1.15	1.15	1.15	1.15	1.15	1.15	1.15	1.15	1.15	1.15	
χ^2 / ndf	54.28 / 27	54.28 / 27	54.28 / 27	54.28 / 27	54.28 / 27	54.28 / 27	54.28 / 27	54.28 / 27	54.28 / 27	54.28 / 27	54.28 / 27	54.28 / 27	54.28 / 27	54.28 / 27	54.28 / 27	54.28 / 27	54.28 / 27	54.28 / 27	
Constant	186.3 ± 5.7	186.3 ± 5.7	186.3 ± 5.7	186.3 ± 5.7	186.3 ± 5.7	186.3 ± 5.7	186.3 ± 5.7	186.3 ± 5.7	186.3 ± 5.7	186.3 ± 5.7	186.3 ± 5.7	186.3 ± 5.7	186.3 ± 5.7	186.3 ± 5.7	186.3 ± 5.7	186.3 ± 5.7	186.3 ± 5.7	186.3 ± 5.7	
Mean	0.02061 ± 0.02456	0.02061 ± 0.02456	0.02061 ± 0.02456	0.02061 ± 0.02456	0.02061 ± 0.02456	0.02061 ± 0.02456	0.02061 ± 0.02456	0.02061 ± 0.02456	0.02061 ± 0.02456	0.02061 ± 0.02456	0.02061 ± 0.02456	0.02061 ± 0.02456	0.02061 ± 0.02456	0.02061 ± 0.02456	0.02061 ± 0.02456	0.02061 ± 0.02456	0.02061 ± 0.02456	0.02061 ± 0.02456	0.02061 ± 0.02456
Sigma	1.049 ± 0.021	1.049 ± 0.021	1.049 ± 0.021	1.049 ± 0.021	1.049 ± 0.021	1.049 ± 0.021	1.049 ± 0.021	1.049 ± 0.021	1.049 ± 0.021	1.049 ± 0.021	1.049 ± 0.021	1.049 ± 0.021	1.049 ± 0.021	1.049 ± 0.021	1.049 ± 0.021	1.049 ± 0.021	1.049 ± 0.021	1.049 ± 0.021	1.049 ± 0.021

Preshower detector

